High-resolution broadband Brillouin scattering study of antiferroelectric phase transition in $CsBi(MoO_4)_2$

M. Mączka
Institute of Low Temperature and Structure Research, Polish Academy of Sciences, P.O. Box 1410, 50-950 Wrocław 2, Poland

J. Hanuza
Institute of Low Temperature and Structure Research, Polish Academy of Sciences, P.O. Box 1410, 50-950 Wrocław 2, Poland and Department of Bioorganic Chemistry, Faculty of Engineering and Economics, University of Economics, Wrocław, Poland

J.-H. Ko and S. Kojima
Institute of Materials Science, University of Tsukuba, Ibaraki 305-8573, Japan
(Received 30 May 2003; revised manuscript received 21 July 2003; published 3 November 2003)

High-resolution Brillouin scattering studies of the antiferroelectric phase transition in $CsBi(MoO_4)_2$ have been performed in the temperature range 360–150 K giving information about the temperature dependence of the acoustic phonons propagating in the [100], [010], and [001] directions as well as the lowest-frequency optic soft phonon. These studies show that the soft phonon remains underdamped up to the transition point where its frequency decreases to zero. Strong anomalies in sound velocity, attenuation, and intensity have been observed for sound waves corresponding to the c_{11}, c_{22}, and c_{44} elastic constants. The coupling between the order parameter and elastic strains is linear quadratic for the c_{11}, c_{22}, and c_{44} elastic constants. In case of the c_{33} and c_{55} elastic constants the coupling is biquadratic, giving rise to a frequency decrease and increase, respectively, of the corresponding acoustic modes below T_c. These results indicate that the phase transition is not purely antiferroelectric, as suggested previously, but occurs most likely to a monoclinic phase (point symmetry C_{2h}) which is simultaneously antiferroelectric and ferroelastic.

DOI: 10.1103/PhysRevB.68.174101 PACS number(s): 78.35.+c, 77.84.−s, 63.70.+h

I. INTRODUCTION

$CsBi(MoO_4)_2$ belongs to the group of layered orthorhombic crystals with the general formula $M^{I}M^{III}(M^{VI}O_4)_2$, where M^{I}=K, Cs, M^{III}=Bi, Dy, Pr, Er, and M^{VI}=Mo, W, which have been of considerable interest due to their rich polymorphism.[1–5] In this group $CsDy(MoO_4)_2$ has been the most extensively studied and a second-order phase transition was discovered at 50 K followed by a first-order cooperative Jahn-Teller phase transition at 42 K.[1] Two phase transitions have also been found in $CsBi(MoO_4)_2$: a second-order one at 325–330 K and a first-order ferroelastic transition at around 125 K.[2,6–8] The second-order phase transition occurs between paraelectric and antiferroelectric phases and above the Curie point T_c the ε_{33} component of the dielectric permittivity follows the Curie-Weiss law with the Curie constant 0.3×10^5 K.[6] The crystal structure of the paraelectric phase is the same as that of $CsPr(MoO_4)_2$ and $CsDy(MoO_4)_2$, i.e., $D_{2h}^3=Pccm$ with two molecules in the unit cell.[9] The crystal structure below T_c has not yet been determined but the reported studies suggest that it may also be orthorhombic, $D_{2h}^8=Pcca$, with doubled a lattice parameter.[2,6–8] Our Raman scattering studies supported the conclusion that the phase transition is connected with a phonon condensation at the [1/2 0 0] point of the Brillouin zone.[10,11] They showed that three modes which appear below T_c exhibit pronounced softening when temperature approaches T_c. Two of these modes, observed at 43 and 35 cm^{-1} at 150 K temperature, become heavily overdamped near T_c. Both of them have a finite frequency at T_c (23 cm^{-1} for the 43-cm^{-1} mode). The third soft mode was observed at unusually low frequency (13 cm^{-1} at 150 K) and was characterized by unusually low damping (less than 3 cm^{-1}).[10] It was not possible to study the temperature dependence of this mode above 270 K by using Raman spectrometry because its frequency was less than 8 cm^{-1} and the mode was obscured by strong Rayleigh scattering. Therefore, we decided to obtain this information by using Fabry-Perot interferometry.

The present paper also reports the studies of acoustic properties of $CsBi(MoO_4)_2$ near T_c by means of Brillouin spectroscopy. It will be shown that this technique gives new information which significantly contributes to an understanding of the phase transition mechanism in this compound. We would also like to emphasize that the present paper is a rare example of scattering studies showing the temperature dependence of a soft mode at extremely low frequency. To the authors knowledge the best known temperature-dependent studies of extremely low-frequency soft optical phonons concern chloranil and $K_3Co_{1-x}Fe_x(CN)_6$ crystals.[12,13] This paper is also a rare example of Brillouin scattering studies of para-antiferroelectric phase transition, especially in layered materials.

II. EXPERIMENT

Single-crystal growth has been described previously.[10]

The Brillouin spectra were obtained with a 3+3 pass tandem Sandercock-type Fabry-Perot interferometer combined with an optical microscope. The free spectral range (FSR) employed was 37.5 GHz (for the study of acoustic phonons) and 375 and 250 GHz (for the study of the soft optical pho-

non). The scattered light from the sample was collected in backscattering geometry. An additional measurement in 90° scattering geometry was performed only at ambient temperature in order to obtain information about n_z refractive index. A conventional photon-counting system and a multichannel analyzer were used to detect and average the signal. The samples were put in a cryostat cell (THMS 600). The sample cell with an *X*-*Y* adjustment was placed onto the stage of an optical microscope (Olympus BH-2) having a *Z* adjustment. The Brillouin spectra were obtained for 1024 channels after 300 time repetitions of accumulation with a gate time of 500 μs for one channel. More details of the experimental setup can be found in our previous paper.[14]

The frequency shifts, half-widths, and intensity of the Brillouin peaks were evaluated by fitting the measured spectra to the convolution of the Gaussian instrumental function with a theoretical spectral line shape that is Lorenzian in form.[15] Sound velocities and corresponding elastic constants were calculated from the measured frequency shifts using the mass density 5.51×10^3 kg/m^3. The refractive index $n_z = 1.91$ was obtained by comparing measurements of Brillouin shifts in backscattering and 90° configuration in the way proposed by Vaughan.[16] Since it is known that Brillouin spectroscopy can be used for the determination of birefringence, the remaining refractive indices were obtained from the Brillouin shifts measured in backscattering geometry.[17] The measured Brillouin shifts for the LA phonon in the $x(zz)x$ and $x(yy)x$ polarization depend on the n_z and n_y refractive indices, respectively.[17] Using the $n_z = 1.91$ value the corresponding sound velocity for the LA phonon traveling in the [100] direction was found to be 3.29×10^3 m/s. Knowledge of this sound velocity and the measured Brillouin shift in the $x(yy)x$ polarization allows us to conclude that the refractive index $n_y = 1.92$. The refractive index $n_x = 1.94$ was obtained in the similar way from the $y(zz)y$ and $y(xx)y$ Brillouin shifts. The refractive indices were taken to be constant in the entire temperature region studied.

III. RESULTS AND DISCUSSION

A. Temperature dependence of the soft optical phonon

The temperature dependence of the soft optical phonon is presented in Fig. 1. Since this mode is underdamped even near T_c, its frequency, damping, and integrated intensity were evaluated by fitting the measured spectra to the convolution of the Gaussian instrumental function with a theoretical spectral line shape that is Lorenzion in form. The obtained values of ω_s and damping as a function of temperature are plotted in Fig. 2.

At $T<T_c$ the temperature dependence of the soft phonon frequency is obtained by a least-squares fitting, which is described by $\omega_s = 1.76(T_c - T)^{0.40}$. This fitting shows that the phonon softens to zero at $T_c = 322$ K. The value of the critical exponent $\beta = 0.40\pm0.01$ is smaller than the predicted mean-field value of 0.5. The temperature dependence of damping is weak (see Fig. 2) and intensity decreases significantly only in a narrow temperature range near T_c.

It is worth noting that the behavior of the 13-cm^{-1} soft mode is different than the behavior of the two other soft

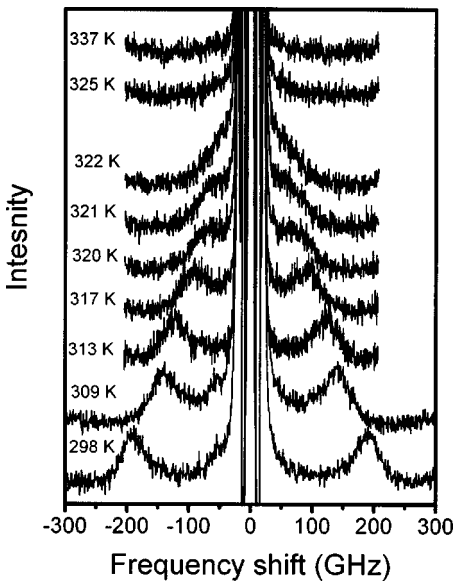

FIG. 1. Development of the optical phonon spectra as a function of temperature.

modes (observed at 43 and 35 cm^{-1} at 150 K) studied by us previously,[10] which showed large finite frequency at T_c (about 23 cm^{-1}) and clear decrease in intensity and increase in damping in a very large range below T_c (more than 100 K). This result indicates that the lowest-frequency soft mode can be attributed to the primary mode whereas the two higher-frequency modes are most likely secondary modes associated with the antiferroelectric distortion in $CsBi(MoO_4)_2$. The unusually low frequency (less than 13

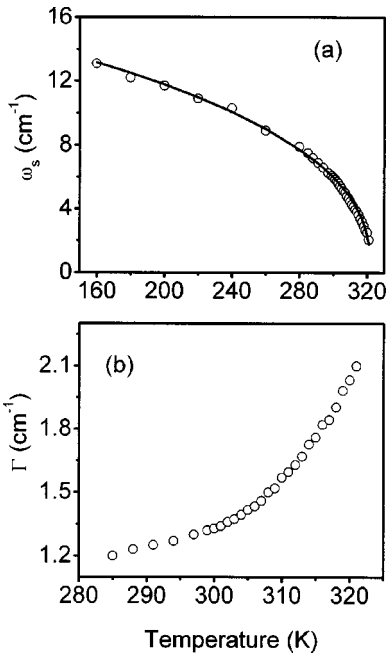

FIG. 2. The temperature dependence of the soft phonon frequency (a) and damping (b). The solid line represents a fit to $\omega = A(T_c - T)^{\beta}$. The data below 280 K are taken from our previous Raman scattering studies (Ref. 10).

TABLE I. Force constants f (in N/m) and frequencies ω (in cm^{-1}) at 350 K of some acoustic and optic modes determined from velocities v (in 10^3 m/s) of TA and LA phonons propagating along [100] direction and corresponding to the c_{55} and c_{11} elastic constants.

v_{LA}	v_{TA}	f_{LA}	f_{TA}	ω_{LA} $k=\pi/a$	ω_{TA} $k=\pi/a$	ω_0^c $k=0$	ω_0^s $k=0$	ω_0^c $k=\pi/a$	ω_0^s $k=\pi/a$
3.29	0.75	53.2	2.8	41.3	9.4	92.2	21.1	82.4	18.8

cm^{-1} at 180 K below T_c) and damping (1.4 cm^{-1} at 300 K) of the lowest-frequency soft phonon suggest that this mode can be attributed either to the translational motions of Cs^+ cations, since these ions interact very weakly with the oxygen atoms, or to antiphase displacements of the layers, so-called rigid layer mode, which corresponds to a zone boundary acoustic mode in the paraelectric phase. In the layered structure frequencies of these modes can be easily calculated with the use of linear chain model and known velocities of acoustic phonons propagating perpendicular to the layers.[18] The application of this model gives the following expressions for sound velocity and frequencies of acoustic and optic modes:

$$v = R[0.5f/(M_1+M_2)]^{1/2}, \tag{1}$$

$$\omega_0 = (2\,f/\mu)^{1/2} \quad \text{for } \mathbf{k}=0, \tag{2}$$

$$\omega_0 = (2\,f/M_1)^{1/2} \quad \text{for } \mathbf{k}=\pi/a, \tag{3}$$

$$\omega_a = (2\,f/M_2)^{1/2} \quad \text{for} \quad \text{for } \mathbf{k}=\pi/a. \tag{4}$$

The parameter f denotes a force constant between the layer composed of cesium ions with mass M_1 and the $[Bi(MoO_4)_2]_{\infty\infty}^-$ layer with mass M_2. The μ is the reduced mass and R is the distance between the same type layers: i.e., R is equal to the a lattice parameter in the D_{2h}^3 structure. Using the measured frequencies for phonons corresponding to the c_{11} and c_{55} elastic constants at 350 K (23.6 and 5.4 GHz, respectively: see next paragraph of this paper), we have calculated the corresponding frequencies (see Table I). The calculations show that the rigid layer mode should be observed around 9 cm^{-1} and the translations of the Cs^+ ions around 19 cm^{-1}. It is, therefore, not possible to discriminate on the basis of the performed calculations whether the observed 13-cm^{-1} mode originates from the transverse acoustic mode or shear optic mode corresponding to translational motions of Cs^+ ions. Since, however, translational motions of weakly polarizable alkali-metal ions give usually rise to weak Raman bands, the strong intensity of the observed soft mode favors the assignment of this mode to the rigid layer mode.

B. Temperature dependence of elastic constants

The structure of $CsBi(MoO_4)_2$ above $T_c = 325$ K is orthorhombic, D_{2h}^3.[9] The elastic stiffness tensor of the orthorhombic group D_{2h} contains nine independent components: i.e., c_{11}, c_{22}, c_{33}, c_{44}, c_{55}, c_{66}, c_{12}, c_{13}, and c_{23}. In the present study only c_{11}, c_{22}, c_{33}, c_{44}, and c_{55} elastic constants have been calculated from the measured frequencies of the longitudinal and transverse modes propagating along the x, y, and z axes. The calculated values of the elastic constants of the D_{2h}^3 phase are presented in Table II. It is worth noticing that the elastic constants c_{44} and c_{55} are very small. The elastic constant c_{66} has even smaller value (frequency of the corresponding acoustic mode is only 3.7 GHz at ambient temperature) and therefore its value in the D_{2h}^3 phase could not be established.

The temperature dependence has been established for LA phonons propagating in the directions [100], [010], and [001] as well as for two transverse phonons propagating in the directions [001] and [100]. The frequency of these phonons correspond to the c_{11}, c_{22}, c_{33}, c_{44}, and c_{55} elastic constants, respectively.

The temperature dependence of the studied phonons shows that the phase transition results in distinct acoustic anomalies (Figs. 3–8). The frequency of the phonon corresponding to the c_{11} constant shows a very clear steplike discontinuity typical for linear-quadratic coupling. The c_{22} and c_{44} constants also show a discontinuous temperature dependence. However, in this case the steplike discontinuity is less clear since critical fluctuations in the order parameter near T_c can lead to an additional downward bending of the c_{22} and c_{44} elastic constants. According to the Landau free-energy expansion, a second-order transition gives a negative contribution to elastic constant change but a first-order transition can give either a positive or negative contribution.[19] The observed negative change in the elastic constants c_{11}, c_{22}, and c_{44} is consistent with the second-order character of the paraelectric-antiferroelectric transition. The phonon corresponding to the c_{55} elastic constant shows a temperature dependence characteristic for the biquadratic coupling below T_c. The unusual feature of the phonon corresponding to the c_{33} elastic constant is a large decrease of its frequency with decreasing temperature (see Fig. 6). The temperature dependence of this phonon can be most likely explained as a result of biquadratic coupling with a negative coupling constant. The other characteristic feature of the studied phonons is a

TABLE II. Calculated velocities of acoustic phonons and elastic constants of $CsBi(MoO_4)_2$ at 350 K.

Wave vector	[100]		[010]	[001]	
Phonon	LA	TA	LA	LA	TA
Velocity (10^3 m/s)	3.29	0.75	3.62	3.39	1.15
Elastic constant	c_{11}	c_{55}	c_{22}	c_{33}	c_{44}
(10^{10} N/m^2)	5.97	0.31	7.21	6.35	0.73

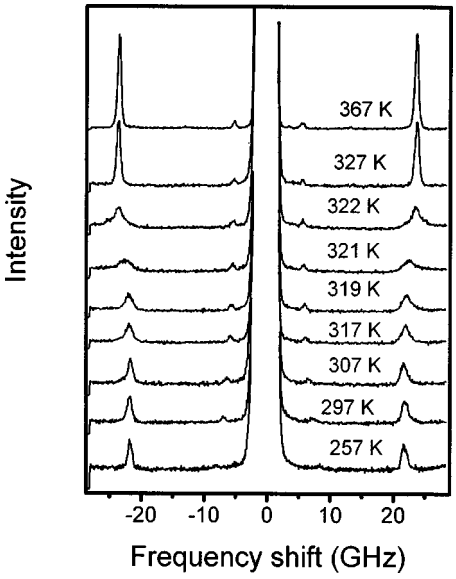

FIG. 3. Example of the temperature dependence of the Brillouin spectra for $CsBi(MoO_4)_2$. The spectra were recorded in the $x(zz+zy)x$ configuration.

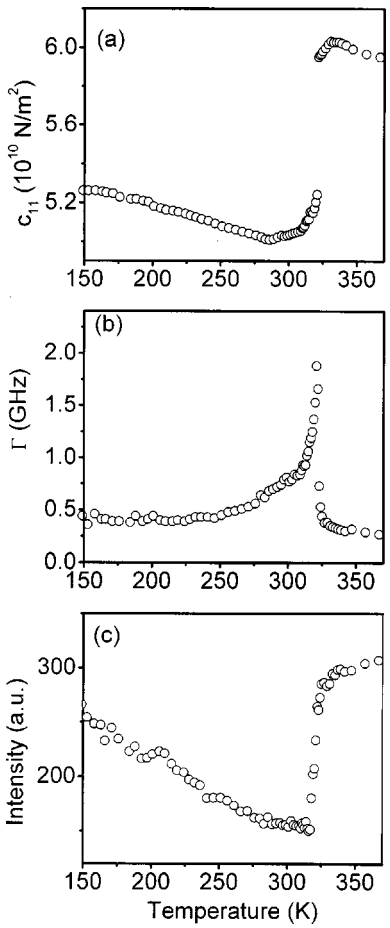

FIG. 4. Temperature variation of the c_{11} elastic constant (a) and the corresponding damping (b) and intensity (c).

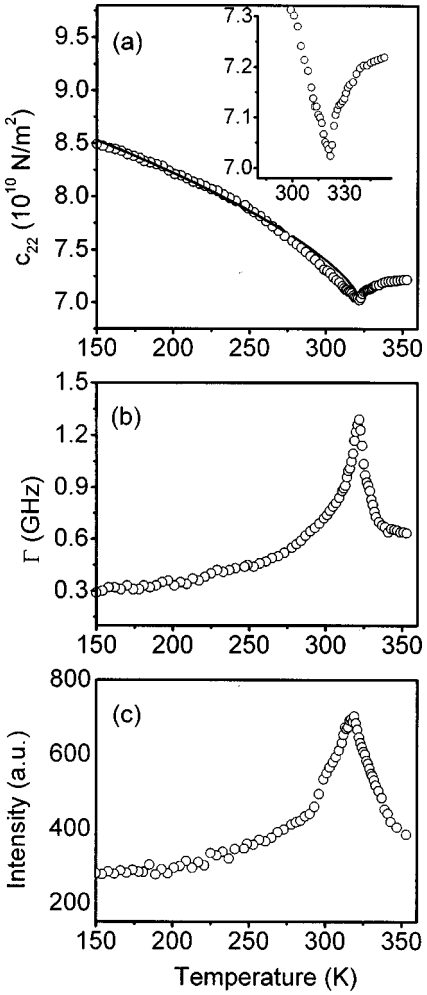

FIG. 5. Temperature variation of the c_{22} elastic constant (a) and the corresponding damping (b) and intensity (c). The solid line represents a fit to Eq. (12). The inset shows details near T_c.

very large increase in damping of the c_{11}, c_{22}, and c_{44} constants at T_c, giving rise to characteristic peaks (see Figs. 4, 5, and 7). The increase in damping for the c_{33} constant is weak (see Fig. 6) and no change can be observed for the c_{55} elastic constant. Finally, as a result of the phase transition a steplike change in scattering intensity (divided by $n(\omega)+1$, where $n(\omega)=1/[\exp(h\omega/k_BT)-1]$ is the Bose-Einstein factor) is observed for the phonons corresponding to the c_{11} and c_{44} elastic constants whereas the c_{22} constant gives rise to maximum intensity at T_c (see Figs. 4, 5, and 7).

The former studies showed that the phase transition at 325 K is antiferroelectric with doubling of the *a* lattice parameter. Since the center of symmetry will always be retained at a pure antiferroelectric transition,[20] the antiferroelectric phase may have D_{2h}, C_{2h}, or C_i symmetry. As mentioned in the Introduction, it has been suggested previously that the low-temperature phase may be described by the $D_{2h}^8=Pcca$ space group: i.e., the phase transition does not lead to any point symmetry breaking but is connected with a decrease of the translational symmetry. Theoretical considerations shows that a *Pccm* to *Pcca* transition with a doubling of the *a* lattice parameter can be induced by a one-dimensional irreducible

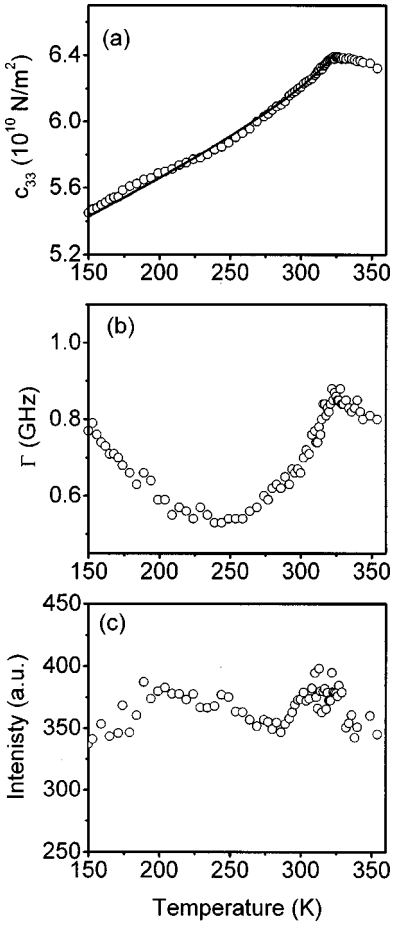

FIG. 6. Temperature variation of the c_{33} elastic constant (a) and the corresponding damping (b) and intensity (c). The solid line represents a fit to Eq. (13).

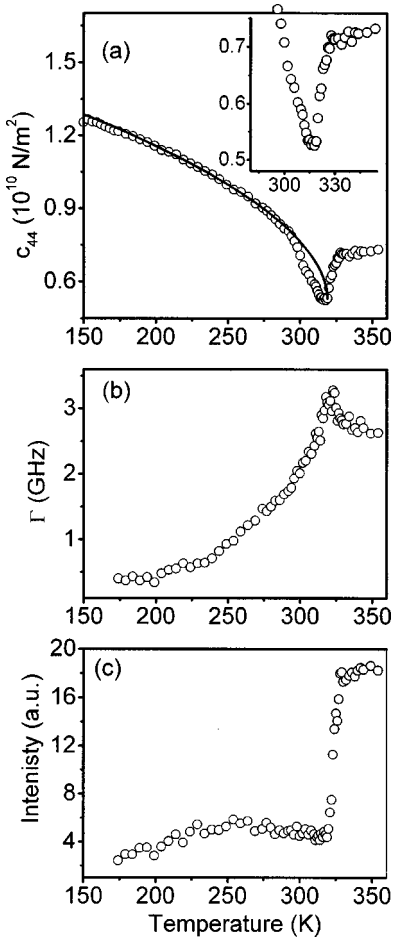

FIG. 7. Temperature variation of the c_{44} elastic constant (a) and the corresponding damping (b) and intensity (c). The solid line represents a fit to Eq. (14). The inset shows details near T_c.

representation τ_3 or τ_8.[21] The symmetry analysis, performed in a way proposed by Aroyo and Perez-Mato,[22] leads to the conclusion that the primary order parameter connected with the *Pccm* to *Pcca* transition may involve antiphase displacements of Cs^+ ions or $[Bi(MoO_4)_2]_{\infty\infty}^-$ layers, in agreement with our scattering studies (see the discussion in the previous paragraph). Moreover, the calculations show that the above-discussed displacements are associated with rotations of the MoO_4^{2-} groups. It seems, therefore, very likely that the previously observed broad bands at 35 and 43 cm^{-1}, which were assigned to librational motions of the MoO_4^{2-} groups and which exhibited significant softening, can be attributed to secondary modes associated with the antiferroelectric distortion.

Although the phase transition mechanism seems to be consistent with the $Pccm \leftrightarrow Pcca$ symmetry change, the observation of linear-quadratic coupling by us for the e_4 strain shows that this transition cannot occur without point symmetry breaking since in this case the linear-quadratic coupling is allowed only for the e_1, e_2, and e_3 strains. Our Brillouin studies show, therefore, that the transition might occur to the C_{2h} structure: i.e., it might be simultaneously antiferroelectric and ferroelastic (the C_i structure can be excluded since in this case steplike discontinuity should be observed also for the c_{55} elastic constant).

In order to discuss acoustic anomalies, we make use of a phenomenological expression for a free energy. The free energy F as a function of temperature, the order parameter η, and the strain components e_i can be written

$$F = F_\eta + F_c + F_i, \tag{5}$$

$$F_\eta = 1/2a(T - T_c)\eta^2 + 1/4B\eta^4 + 1/6D\eta^6, \tag{6}$$

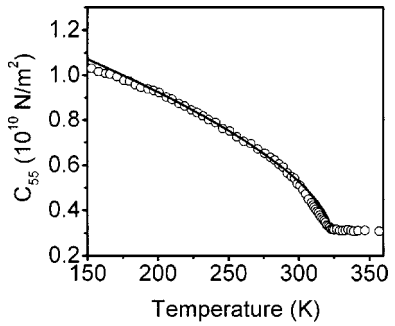

FIG. 8. Temperature variation of the c_{55} elastic constant. The solid line represents a fit to Eq. (15).

TABLE III. Values of the parameters corresponding to the best fits of the data with Eqs. (11)–(15).

Elastic constant	$c_{ii}^0(T_c)$ (10^{10} N/m^2)	δ_i (K^{-1})	$2k_i^2/B$ (10^{10} N/m^2)	A_i'	h_i (10^{10} N/m^2)	β
c_{11}	6.06	4.3×10^{-4}	1.13	~0	-	-
c_{22}	7.24	-	0.22	0.049	-	0.33 ± 0.02
c_{33}	6.40	3.1×10^{-4}	0	0	-0.0086	0.42 ± 0.02
c_{44}	0.73	~0	0.20	0.048	-	0.27 ± 0.03
c_{55}	0.31	4.1×10^{-4}	0	-	0.015	0.31 ± 0.01

$$F_c(e_i,\eta)=\sum_{i=1}^{4} k_i e_i \eta^2+1/2\sum_{i=1}^{6} h_i e_i^2 \eta^2 + 1/2\sum_{1\leqslant i<j\leqslant 4} h_{ij} e_i e_j \eta^2+1/2 h_{56} e_5 e_6 \eta^2, \quad (7)$$

$$F_i(e_i)=1/2\sum_{i=1}^{6} c_{ii}^0 e_i^2+\sum_{1\leqslant i<j\leqslant 4} c_{ij}^0 e_i e_j + c_{56}^0 e_5 e_6. \quad (8)$$

In the static approximation, if we neglect the fluctuations, the effective elastic constants $c_{ii}(T)$ can be written[23]

$$c_{ii}(T)=c_{ii}^0 \quad \text{for} \quad T>T_c, \quad (9)$$

$$c_{ii}(T)=c_{ii}^0-2k_1^2B+(2h_i+4k_iA_i)\eta_0^2 \quad \text{for} \quad T<T_c, \quad (10)$$

where c_{ii}^0 is the bare elastic constant, η_0 is the equilibrium value of the order parameter, and $A_i=2h_ik_i/c_{ii}^0B+k_iD/B^2$. Since the linear-quadratic coupling is not observed for the e_3 and e_5 strains, in the following discussion we take $k_3=0$ and $k_5=0$. With these assumptions, the temperature dependences of the c_{11}, c_{22}, c_{33}, c_{44}, and c_{55} elastic constants below T_c are

$$c_{11}(T)=c_{11}^0(T)-2k_1^2/B+A_1'\eta_0^2, \quad (11)$$

$$c_{22}(T)=c_{22}^0(T)-2k_2^2/B+A_2'\eta_0^2, \quad (12)$$

$$c_{33}(T)=c_{33}^0+2h_3\eta_0^2, \quad (13)$$

$$c_{44}(T)=c_{44}^0(T)-2k_4^2/B+A_4'\eta_0^2, \quad (14)$$

$$c_{55}(T)=c_{55}^0+2h_5\eta_0^2, \quad (15)$$

where $A_i'=2h_i+4k_iA_i$.

In addition, we take into account the thermal expansion of the $CsBi(MoO_4)_2$ crystal which introduces a linear temperature dependence term in $c_{ii}^0(T)$:

$$c_{ii}^0(T)=c_{ii}^0(T_c)[1+\delta_i(T_c-T)]. \quad (16)$$

The resulting values of the parameters corresponding to the best fits of the data with Eqs. (11)–(16) are presented in Table III. The fitting shows that the data can be reasonably well approximated by Eqs. (11)–(16), except for the 20–30 K range near T_c. The significant difference between the experimental and approximated data near T_c is especially well visible for the c_{22} and c_{44} elastic constants (see Figs. 5 and 7) and can be attributed mainly to the fluctuations of the order parameter. The largest jumps in c_{ii} are observed for the c_{44} ($2k_4^2/Bc_{44}^0=0.27$) and c_{11} ($2k_1^2/Bc_{11}^0=0.19$) elastic constants whereas the jump of the c_{22} constant is only 0.03. Note that the A_1' parameter is approximately zero, indicating that the h_1 and D have also approximately zero values. This result shows that the term $1/6D\eta^2$ in the free-energy expansion [Eq. (6)] can be dropped. It is also worth noting that the shear elastic constants c_{44} and c_{55} exhibit a very large increase of their values with decreasing temperature (see Figs. 7 and 8). The analysis shows that the β parameter is around 0.3 for all elastic constants except for c_{33}. This value is similar to that found for the c_{11} elastic constant in K_2SeO_4 near the transition from the hexagonal to orthorhombic, incommensurate phase.[23] It is, however, significantly lower than the value obtained from the soft mode analysis. These results show that the temperature dependence of the order parameter differs significantly from mean-field behavior. The origin of this behavior is not known but it can indicate that the nature of the phase transition is close to tricritical since in such a case η should be proportional to $(T_c-T)^{0.25}$. Another possible explanation is that the higher-order terms play important role in the interactions between the order parameter and strains. It is also worth noting that similar temperature dependence is often observed when a transition occurs into an incommensurate phase. For example, the analysis performed for K_2SeO_4 showed that the temperature dependence can be approximated by a power low with $\beta=0.5$ near T_i whereas further away from the transition it resembles a power low with $\beta=0.25$.[24]

Let us now discuss the damping and fluctuations of the order parameter. There are two major mechanisms of damping. First, the damping is caused by coupling of a strain to the square of the order parameter fluctuations.[19,24–27] This type of coupling brings about the critical damping both below and above T_c. As a result the observed anomaly is symmetric. The second mechanism is connected to bilinear coupling of strain and order parameter fluctuations.[19,24–27] When the order parameter does not correspond to the Brillouin zone center, this contribution to the damping vanishes above T_c. As a result the observed anomaly is strongly asymmetric. Our studies show the presence of a symmetric and strong anomaly for the c_{22} elastic constant (see Fig. 5). The obtained results show, therefore, that this elastic constant couples strongly to the square of the order parameter fluctuations. This mechanism seems to be also very important for

the c_{44} elastic constant. The c_{33} elastic constant also couples to the square of the order parameter fluctuations but this coupling is much weaker than that observed for the c_{22} and c_{44} constants. In case of the c_{11} elastic constant the coupling to the square of the order parameter fluctuations seems to be negligible, as evidenced through a very weak change in damping above T_c. The observed anomaly can be, therefore, attributed to the bilinear coupling between the strain and order parameter fluctuations. The last measured elastic constant, c_{55}, does not show any anomaly in damping. This behavior is consistent with the observed biquadratic coupling since in such a case no contribution to the damping should be observed from the order parameter fluctuations.[24]

Finally, it is worth noting that the studies show steplike intensity change for the c_{11} and c_{44} elastic constants, broad peak for the c_{22} elastic constant and nearly no change for the c_{33} and c_{55} constants. The steplike decrease in intensity at a phase transition is sometimes observed due to formation of microdomains which cause significant deterioration of crystal optical quality.[28,29] In the present case the steplike decrease in intensity at T_c due to deterioration of the crystal optical quality is very unlikely since we could not observe any changes in the crystal transparency below T_c and the simultaneous measurement of the c_{11} and c_{55} or c_{44} and c_{33} elastic constants showed large anomaly in intensity for only one component of each pair. Therefore, the observed changes can most likely be attributed to coupling between the order parameter and strains. A very similar steplike anomaly in intensity was observed previously for a TA phonon in $BaMnF_4$.[30] The steplike change in intensity indicates that the phase transition leads to discontinuous changes in p_{31} and p_{23} elasto-optic (Pockels) coefficients. The mechanism of this temperature behavior has yet to be interpreted. In case of the c_{22} elastic constant the anomaly in intensity resembles that of damping. The observed peak can be, therefore, most likely attributed to fluctuations of the order parameter which give rise to anomalous scattering intensity increase near T_c.

IV. CONCLUSIONS

The performed studies have shown that the soft mode associated with the primary order parameter softens to zero at T_c and remains underdamped even at temperatures very close to T_c. The Brillouin studies, showing the jump decrease in the c_{11}, c_{22}, and c_{44} elastic constants at T_c typical for linear-quadratic coupling, are consistent with the second-order character of the phase transition occurring with doubling of the *a* lattice parameter. However, the present studies show that the mechanism of this transition is more complicated than previously assumed. In particular, the appearance of the jump in the transverse sound velocity c_{44} indicates that as a result of the phase transition e_4 spontaneous strain appear; i.e., the phase transition is both antiferroelectric and ferroelastic. The low-temperature phase cannot be described by the space group *Pcca*, as previously suggested, but is most likely monoclinic with a point group C_{2h}. The observation of the jump for the c_{44} elastic constants indicates that the axis $C_2 \| x$ is retained below T_c. The transition into a monoclinic structure with the doubling of the *a* lattice parameter can be induced by a number of irreducible representations and, therefore, more experimental data, especially x-ray studies below T_c, are necessary to establish the structure of the low-temperature phase. Without knowledge of the crystal structure below T_c, it is not possible to discuss the detailed mechanism of the phase transition. The symmetry analysis and experimental data allow us, however, to conclude that the phase transition involves displacements of the Cs^+ ions or, more likely, $[Bi(MoO_4)_2]_{\infty\infty}^{-}$ layers as well as reorientations of the MoO_4^{2-} tetrahedra.

ACKNOWLEDGMENTS

This work was done as a part of Poland-Japan project and it was partly supported by the Polish Committee for Scientific Research, Grant No. 7 TO9A 020 21. Dr. M. Mączka acknowledges Tsukuba University for support of his stay in Japan.

[1] V. I. Fomin, V. P. Gnezdilov, V. V. Eremenko, and N. M. Nesterenko, Sov. Phys. Solid State **31**, 871 (1989), and references therein.
[2] A. I. Zvyagin and V. I. Kutko, Fiz. Nizk. Temp. **13**, 537 (1987).
[3] M. T. Borowiec, V. Dyakonov, A. Jedrzejczak, V. Markowich, A. Nabialek, A. Pavlyuk, S. Piechota, A. Prokhorov, and H. Szymczak, Solid State Commun. **102**, 627 (1997).
[4] M. I. Leask, O. C. Tropper, and M. L. Wells, J. Phys. C **14**, 3481 (1981).
[5] D. Mihailovic, J. F. Ryan, and M. C. K. Wiltshire, J. Phys. C **20**, 3047 (1987).
[6] A. Brilingas, I. Grigas, A. Gurskas, A. I. Zvyagin, V. Kalesinskas, and L. N. Pelich, Sov. Phys. Solid State **22**, 2039 (1980).
[7] L. N. Pelich and A. I. Zvyagin, Sov. Phys. Solid State **20**, 1106 (1978).
[8] S. Stokka and V. Samulionis, Phys. Status Solidi A **67**, K89 (1981).
[9] P. V. Klevtsov and V. A. Vinokurov, Kristallografiya **18**, 1192 (1973).
[10] M. Maczka, S. Kojima, and J. Hanuza, J. Phys.: Condens. Matter **10**, 8093 (1998).
[11] M. Maczka, S. Kojima, and J. Hanuza, J. Phys. Chem. Solids **61**, 735 (2000).
[12] A. Girard, Y. Delugeard, C. Ecolivet, and H. Cailleau, J. Phys. C **15**, 2127 (1982).
[13] A. Yoshihara, M. Kurosawa, and Y. Morioka, Jpn. J. Appl. Phys., Part 1 **36**, 3318 (1997).
[14] F. M. Jiang and S. Kojima, Appl. Phys. Lett. **77**, 1271 (2000).
[15] W. F. Oliver, C. A. Herbst, S. M. Lindsay, and G. H. Wolf, Rev. Sci. Instrum. **63**, 1884 (1992).
[16] J. M. Vaughan, *Fabry-Perot Interferometer: History, Theory, Practice, and Applications* (Hilger, Bristol, 1989).
[17] T. C. Chey, S. Lee, Y.-S. Yu, and S.-C. Kim, Proc. SPIE **3425**, 196 (1998).
[18] *Vibrational Spectra and Structure*, edited by J. R. Durig (Elsevier Science, Amsterdam, 1985), Vol. 14.

[19] W. Rehwald, Adv. Phys. **22**, 721 (1973).
[20] R. Blinc and B. Žeks, *Soft Modes in Ferroelectrics and Antiferroelectrics* (North-Holland, Amsterdam, 1974).
[21] P. Toledano and J.-C. Toledano, Phys. Rev. B **25**, 1946 (1982).
[22] M. I. Aroyo and J. M. Perez-Mato, Acta Crystallogr., Sect. A: Found. Crystallogr. **54**, 19 (1998).
[23] M. Cho and T. Yagi, J. Phys. Soc. Jpn. **50**, 543 (1981).
[24] J. J. L. Horikx, A. F. M. Arts, J. I. Dijkhuis, and H. W. De Wijn, J. Phys.: Condens. Matter **1**, 5767 (1989).
[25] S. Yoshida, Y. Tsujimi, and T. Yagi, J. Phys. Soc. Jpn. **64**, 5 (1995).
[26] T. Hikita, P. Schnackenberg, and V. H. Schmidt, Phys. Rev. B **31**, 299 (1985).
[27] I. Hatta, M. Hanami, and K. Hamano, J. Phys. Soc. Jpn. **48**, 160 (1980), and references therein.
[28] M. H. Kuok, S. C. Ng, H. J. Fan, M. Iwata, and Y. Ishibashi, Solid State Commun. **118**, 169 (2001).
[29] M. Maczka, J.-H. Ko, S. Kojima, A. Majchrowski, and J. Hanuza, J. Raman Spectrosc. **34**, 371 (2003).
[30] D. J. Lockwood, A. F. Murray, and N. L. Rowell, J. Phys. C **14**, 753 (1981).